❏   700

Performance Analysis of Fiber Attenuation in Passive Optical Networks

Augustus E. Ibhaze[1], Adekunle O. Gbadebo[2], Akinwumi A. Amusan[3], Samuel N. John[4]
[1, 2, 3] Department of Electrical and Electronics Engineering, University of Lagos, Nigeria
[4]Department of Electrical and Electronics Engineering, Nigerian Defence Academy, Nigeria

Article Info	ABSTRACT
	The introduction of Fiber Optics cables in broadband Internet distribution has been a game changer in bulk capacity delivery, speed, reliability and penetration. However, the uncurbed incessant existence of cuts and failures have threatened the growth of Internet connectivity as a whole. In this work, the impact of fiber cuts is investigated using a hybrid approach, encompassing both real-world data from a live GPON network and simulations using OptiSystem 12 for FTTH GPON scenarios. Fiber cuts and failures are emulated by introducing varying attenuation levels in the simulated network's feeder cable section within OptiSystem 12, while in the live GPON network, the attenuation is induced by introducing wrap bends in the last-mile patch cord. The findings reveal a consistent pattern in both simulated and live data for both downstream and upstream traffic scenarios. As attenuation levels increased, there was a corresponding decline in Q-factor, Eye Height, and optical power, coupled with a concurrent rise in the minimum BER. Thus, in the most severe scenario, fiber cuts can result in service degradation and eventual service outage. To mitigate this issue, the implementation of a type-B PON protection system with a wireless auto-failover technique is proposed. Adoption and deployment of the proposed technique and deliberate maintenance measures alongside thorough supervision are suggested to be possible solutions to fiber cuts in metropolitan parlance.

Corresponding Author:

Dr. Augustus Ehiremen Ibhaze,
Department of Electrical and Electronics Engineering,
University of Lagos,
Faculty of Engineering, University of Lagos, Nigeria.
Email: eibhaze@unilag.edu.ng

1. INTRODUCTION

The telecommunications network has experienced an unprecedented need for bandwidth due to the extensive development of information technology and broadband applications. Fiber optics, which takes advantage of current optical fiber communication technology, is quickly becoming the most effective way to increase network capacity while keeping costs low. Broadband technology allows for speedy data transfer on the Internet, and networks were created to improve this technology with better data rates and improved quality of service [1] [2]. The backbone to these network are majorly fiber optics. For instance, Nigeria has five Submarine fiber optics cable networks which provide a broadband capacity of over 27 Tbps for the country's connection to the world. Despite this, there is still relatively low subscriber-level Internet broadband penetration and the fiber optic networks are mainly concentrated in urban areas. Additionally, private telecommunications companies that deploy mobile services have the highest number of fiber optic deployments, prioritizing solutions for their network challenges [3].

Optical fiber was initially developed in the 1970s, but it wasn't until the early 1980s that it saw large-scale commercial use. By the 1990s, fiber networks had revolutionized telecommunications. Advancements in technology continued at a rapid pace, surpassing actual demand by the end of 2000. The first commercial fiber

optic connection was made in Long Beach California in April 1977, initially capable of transmitting at a rate of 6 Mbps. However, this speed has since been significantly improved to over 3.2 Tbps, resulting in a million-fold increase in speed. Optical fiber operates using light as the transmission medium, and consists of a laser or LED light source, an optical glass fiber for transmitting data, and an optical receiver that converts the light pulse back into an electrical pulse [4].

As mobile broadband internet usage continues to increase in globally, largely driven by the use of smartphones and other mobile devices, there is an imperative to also improve internet access through fixed broadband. The International Telecommunication Union's statistics show that Nigeria's internet penetration rate is 6%, which is relatively low. A review of broadband internet penetration in Nigeria reveals that Nigeria's broadband penetration rate is still relatively low compared to other regions globally, with Africa having a broadband penetration rate of 19% [5]. The past few years have seen unprecedented growth in the fiber optic communications industry, accompanied by swift technological advancements [6]. The telecommunications industry widely acknowledges fiber optics network technology as the fastest and most commonly-used means of transmitting backhaul. It has sufficient capacity and capability to fulfil the telecom needs of present-day customers [7]. The number of active voice subscriptions in Nigeria rose from 1.84 million in 2019 to 2.05 million by December 2020. This indicates an increase of 1.9 million subscriptions, which is a total of about 10.78% growth within the period considered. Moreover, the country's teledensity went up from 96.76% in December 2019 to 107.18% by December 31st 2020. The broadband penetration also saw progress, as it increased from 37.80% in December 2019 to 45.02% by December 2020. Correspondingly, broadband subscriptions surged from 72,153,824 subscriptions in December 2019 to 89,941,222 subscriptions as of December 2020 [8]. These increasing numbers give more credence to the rate of technological growth in Nigeria and a technology-growing nation. This growth, however, is challenged by the major problem of outages on the delivery and maintenance of the fiber optics mode of the broadband delivery and coverage expansion – fiber cuts.

Despite advanced optical technology [9] [10], today's fiber networks are still vulnerable to damage because they are housed in cables. Even with appropriate protection measures, when deploying a cable that spans 100,000 miles, it is prone to damage quite frequently, with estimates suggesting that a single mile can operate for about 228 years before being damaged. While this estimate may initially sound reassuring, it implies that on average, there may be more than one cut per day on the 100,000 installed route miles. Such failures may be more common during construction activities, leading to some days where multiple cuts occur [11]. According to [12], fiber cuts may be categorized based on the type of deployment. There are causes peculiar to cuts in aerial deployments, underground or subsurface fiber cable deployment and causes peculiar to both modes of deployment. In Crawford's investigation, a total of 131 underground or sub-surface cases were analyzed, 71% were accounted to dig-ups, followed by process errors at 7%. A dig-up refers to harm inflicted upon fiber optics cable while penetrating the ground for various activities, such as sign placement, road grading, trenching, and installing or fixing sub-surface facilities. Process error damage pertains to cuts triggered by telecommunication workers while doing maintenance or installation tasks, but does not encompass procedural errors resulting in excavation disruptions. Floods, non-dig up excavations and vehicular accidents ranks bottom threat of about 2% each.

According to [11], an outage and a cut in an optical cable refer to events resulting from actual failures, where a communication cable is damaged and disrupts normal operations, usually requiring emergency repair. Therefore, the fiber cut phenomenon in the telecommunications industry involves interrupting an active optical cable connected to a network element due to specific activities near the location(s) of the deployed cables. This phenomenon often causes network outages, and the impact on network quality (voice and data traffic), cost of operation, and revenue margin depends on the number and location of cuts. This issue has a significant effect on the telecom industry's service delivery and financial performance [7]. This research work is poised at analysing the effects of these fiber cuts and failures by using live and simulated data from Service providers in Nigeria.

2.   RESEARCH METHOD

A GPON network is designed using the OptiSystem 20 simulation software. The GPON network is to demonstrate a basic GPON fiber network where fiber cuts and failures are simulated by altering the attenuation on the feeder cable section of the outside plant infrastructure. Six iterations were conducted, each with a different attenuation value. The impact of the increasing attenuation value on the feeder cable section was observed in BER analysis and Eye Diagram which revealed a corresponding change in the minimum BER, Eye height, Q-factor and Optical Power. The feeder cable was 5.4 km long and the attenuation on the fiber cable was varied six times between values of 0.1 and 5 dB/km. Figure 1 depicts the design of the GPON Network for Simulation. The Optical Line Terminal (OLT) of the GPON network is designed with Upstream

and downstream optical components. The upstream Transmitter operates at a wavelength of 1490nm with a power of 3 dBm and modulation type of Non-Return-to-Zero (NRZ). The downstream pump runs at a wavelength of 1239 nm at a power of 980mW. The upstream pump runs at a frequency of 1427nm and at a power of 370 mW. The OLT also has an Ideal Mux, buffer selector, butterworth optical fiber, photodetector and low pass filter (LPF) at a cutoff frequency scaled by a factor of 0.75 and a 3R signal generator. The Downstream BER Analyzer is connected to the 3R signal generator from which the BER data is obtained. The Optical distribution Frame (ODF) contains the feeder fiber and the Remote Nodes (RN). The directional fiber cable then goes into a 1:64 GPON splitter. A power meter is introduced on one of the splitter outputs to measure the Optical power upstream.

The Optical Network Unit (ONU) represents the client-end fiber receiver. It comprises of a photodetector PIN, a Low Pass Bessel Filter with a cutoff frequency scaled by a factor of 0.75, and a 3R signal regenerator all for the upstream signal. The Upstream signals are measured through the aid of a BER Analyzer that terminates on the 3R regenerator. The Downstream signal is launched with a transmitter on 1310 nm, a power of 0 dBm also running the Non-Return-to-Zero (NZR) modulation type. The GPON design for the experiment on a simulated network in the bid to observe the impact of fiber failures on the performance of network/Internet service provided by a fiber optics cable system is shown in Figure 1.
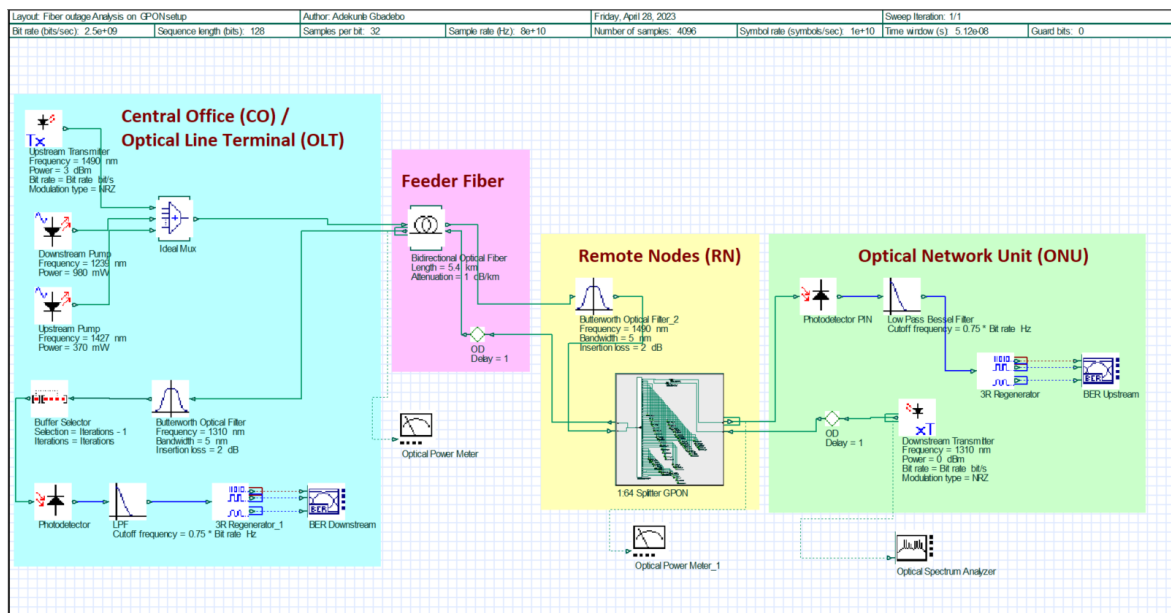

Figure 1. Simulated GPON Network for Fiber Cut Evaluation

The simulated results are validated by comparing the network performance with a live network on which fiber cut was induced. The algorithmic flowchart for the implementation of this research method is depicted in Figure 2.

The performance metric for the network link are the BER and Q-Factor for which the BER, assuming Gaussian noise with the standard deviations σ_0 and σ_1 is given by [13]:

$$P_e = \frac{M}{N+M} P_{e0} + \frac{N}{N+M} P_{e1} \tag{1}$$

where P_{e0} and P_{e1} are the probabilities of the symbols, M is the number of samples for the logical 0, and N is the number of samples for the logical 1.

also, P_{e0} and P_{e1} are

$$P_{e0} = \frac{1}{2} erfc \left(\frac{S-\mu_0}{\sqrt{2}\sigma_0} \right) \tag{2}$$

$$P_{e1} = \frac{1}{2} erfc \left(\frac{\mu_1-S}{\sqrt{2}\sigma_1} \right) \tag{3}$$

where μ_0, μ_1, σ_0, and σ_1 are average values and standard deviations of the sampled values respectively, and S is the threshold value.

The simple Gaussian approximation can be enhanced by averaging the separately estimated BER for different sampled symbols [14]. For M sample values for the logical 0 and N sampled values for the logical 1, the corresponding error rates are given by:

$$P_{e1} = \frac{1}{2N} \sum_{i=1}^{N} erfc \left(\frac{\mu_{1i}-S}{\sqrt{2}\sigma_{1i}} \right) \tag{4}$$

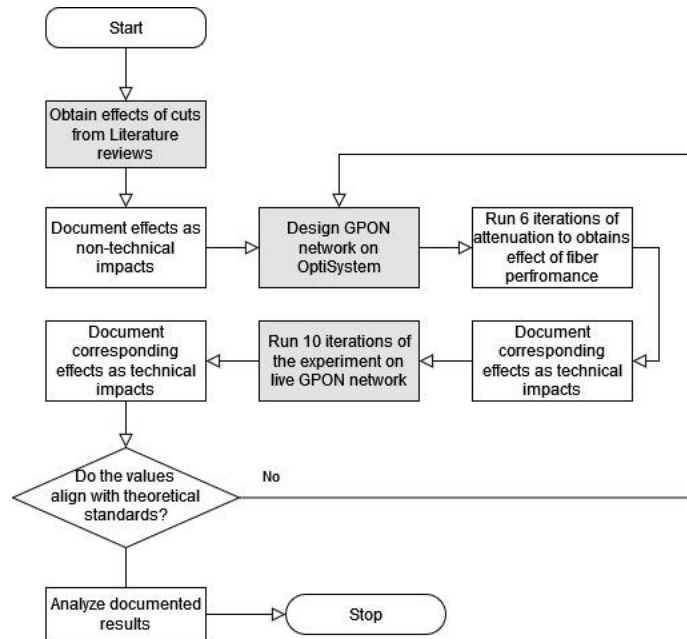$$P_{e0} = \frac{1}{2M} \sum_{i=1}^{M} erfc\left(\frac{S-\mu_{0i}}{\sqrt{2}\sigma_{0i}}\right) \tag{5}$$

Figure 2. Decision flowchart for fiber cut analysis

If the signal is mixed with the noise, the average Gaussian method is modified to estimate the average error patterns, then, the BER is given by [15]:

$$P_e = \sum_{i=1}^{8} \frac{N_P}{N} erfc\left(\frac{\mu_i-S}{\sqrt{2}\sigma_i}\right) \tag{6}$$

where N_P is the number of occurrences of any pattern, N is the total number of patterns, μ_i and σ_i are average values and standard deviations for the sampled values for each pattern respectively, and S is the threshold value.

Since the average Gaussian method can estimate the BER per bit or per pattern, the worst-case Gaussian searches for the min BER for each bit or pattern rather than evaluate the average values. The Chi-Squared estimator is adequate for received signals with non-Gaussian statistics. The analyzer will estimate the Chi-Squared parameters after statistical analysis of the received signal [16] [17] [18]. The probability of error is estimated according to:

$$P_e = \frac{M}{N+M} \int_{S}^{\infty} f_{x^2}(x|0) + \frac{N}{N+M} \int_{-\infty}^{S} f_{x^2}(x|1) \tag{7}$$

The model can also evaluate the average error pattern and the worst case pattern. The measured method will count the errors directly e.g. the total number of marks below spaces divided by the total number of bits. The Q-factor from BER is estimated numerically by:

$$P_e = \frac{1}{2} erfc\left(\frac{Q}{\sqrt{2}}\right) \tag{8}$$

where the Q-factor is estimated by:

$$Q = \frac{|\mu_1-\mu_0|}{\sigma_1+\sigma_0} \tag{9}$$

The eye height is evaluated by [14]:

$$E_H = (\mu_1 - 3\sigma_1) - (\mu_0 + 3\sigma_0) \tag{10}$$

The eye amplitude is given by:

$$E_A = \mu_1 - \mu_0 \tag{11}$$

The eye closure is:

$$E_c = min(V_1) - max(V_0) \tag{12}$$

where $min(V_1)$ is the minimum value of the amplitude for the marks and $max(V_0)$ is the maximum value for the amplitude of the spaces.

The eye-opening factor is evaluated by:

$$E_0 = \frac{(\mu_1-\sigma_1)-(\mu_0-\sigma_0)}{(\mu_1-\mu_0)} \tag{13}$$

The extinction ratio is given by:

$$E_R = \frac{\mu_1}{\mu_0} \tag{14}$$

For the user defined threshold, the input file, given by the parameter measured threshold filename, is formatted with two items per line, the time and threshold amplitude. Time is given in ratio of the bit period, and amplitude is given in arbitrary units (voltage or current). An experiment was conducted on a GPON live network comparable to the simulated network. Attenuation was induced by applying wrap bends on the last mile patch cord. Turns of the fiber cable infers a type of failure in bends and poor cable management. The goal of this method was to obtain the effect of fiber cut or failures in form of attenuation of a GPON fiber cable network. Attenuation was induced by causing bends on the fiber patch cord on the last mile to the ONU. These bends induced bending loss which in turn causes attenuation. Attenuation as revealed in the literature is a major effect on the quality of service. Figure 3 shows the Fiber ONU used in this experiment and the termination of the patch cord to the ONU. The bends were measured by wrapping turns on cylindrical pole of 60mm diameter. It is expected that the more the turns around the cylindrical pole, the Rx power loss changes due to bending losses thereby causing attenuation. Figure 4 reveals the method of inducing bending losses on the network for this experiment. The ISP network was a GPON network with the following core elements: Optical Line Terminal (OLT) – A 8 slot by 32 port Raisecom GPON OLT at the central Office; Optical Distribution Frame (ODF) which includes the Feeder fiber (The 64 core fiber cable and distribution cabinet) and a Remote Node (it contains 2 sections of 1:8 passive splitter); and an Optical Network Terminal – A 4 port Raisecom GPON ONU at the user premise.

Figure 3. Bottom view of Fiber ONU device showing patch cord termination

Figure 4. Inducing fiber failure through fiber cable bending over a cylindrical object

3. RESULTS AND DISCUSSION

The simulated GPON Network designed on OptiSystem 20 is described in Figure 1. The results of 6 different iterations of the attenuation constant at the 5.4 km feeder cable section on downstream and upstream is captured in Tables 1 to 2 and Figures 5 to 11.

Table 1. Parameter reading OLT downstream with 3 dBm transmit power and NRZ modulation

S/N	Attenuation (dB/km)	Max Q Factor	Min BER	Eye Height	Threshold	Optical Rx Power (dBm)
1	0.1	57.4532	0	6.56487e-05	2.25069e-05	-26.650
2	0.5	18.9719	0	1.77043e-05	1.03237e-05	-28.963
3	1	5.79152	0	2.9807e-06	2.91524e-06	-31.190
4	1.5	2.07807	0.015748	-9.5485e-07	1.12507e-06	-32.065
5	2.0	0.719302	0.19685	-2.54121e-06	4.10718e-07	-34.150
6	5.0	0.0706591	0.472441	-3.24771e-06	-6.8394e-08	-50.506

Table 2. Parameter reading OLT upstream with 0 dBm transmit power and NRZ modulation type

S/N	Attenuation (dB/km)	Max Q Factor	Min BER	Eye Height (AU)	Optical Rx Power (dBm)
1	0.1	9.64379	2.59178e-22	8.01221e-06	-20.872
2	0.5	4.94287	3.84897e-07	2.24442e-06	-23.853
3	1.0	2.43216	0.00749335	-6.28109e-07	-27.263
4	1.5	1.20629	0.112672	-1.85165e-06	-30.446
5	2.0	0.676554	0.249342	-2.53787e-06	-33.405
6	5.0	0.160096	0.429667	-3.33803e-06	-38.271

Figures 5 and 6 shows the Eye diagram results of the varying attenuation value both on the upstream and downstream of the GPON network. Figure 7 shows the Q-factor results of the varying attenuation value both on the upstream and downstream of the GPON network. Figure 8 shows the minimum BER results of the varying attenuation value on the feeder fiber cable both on the upstream and downstream of the GPON network. Graphs of these relationships are shown in Figure 9 and 10.

From Table 1, a decreasing maximum Q Factor from 57.45 at 0.1dB/km attenuation to 18.97 maximum Q factor on 0.5 dB/km is observed in the case of downstream. Though the decrease is not constantly proportional to the corresponding increase across the six iterations, it can be confirmed that a persistent pattern of reduction is observed on the maximum Q factor for every increase in attenuation. This implies that the quality of signal drops with an increase in attenuation. A similar pattern is observed on the upstream data in Table 2. This is portrayed by the inversely proportional graphs in Figure 7.

Minimum BER results in Table 1 and Table 2 slightly differ as the downstream data (Table 1) maintains a constant zero on the first three iterations. This behavior is normal as there is little or no error with attenuation less than 1dB/km on a 5.4km cable length based on calculations in Equation 3.8. From the fourth iteration till the sixth with attenuation ranging from 1.5dB/km to 5dB/km, a constantly increasing Min BER was observed. This confirms that error rates increases with an increase in attenuation. On the other hand, upstream data captured in Table 2 followed a similar pattern of little or no BER till its' appreciable increase, showing a directly proportional relationship between attenuation and the minimum BER. The graphs in Figure 8 shows this relationship.

An inversely proportional relationship is observed with the Eye Heights both on the upstream and downstream data in Table 1 and Table 2. This means that the more the attenuation, the smaller the Eye Height. This relationship as depicted in Figure 9 confirms the theory that the smaller the eye height, the poorer the optical signal at the receiver. The relationship between the Eye Height and attenuation is futher depicted in Figures 5 and 6.

The significant depreciation of the eye heights from 8.01e-06 to -3.33e-06 as the attenuation increases from 0.1 to 5dB/km as also portrayed in Figures 5 (downstream) and Figure 6 (upstream) reveals the depreciation of the signal at the receiver. From the Eye diagrams it is observed that there is a gradual disappearance of the eye opening. Figure 5a shows a very clean signal with a well opened eye while it was observed that the eye closes gradually across Figures 5b to Figure 5d till it completely disappears to a very much scrambles and distorted signal in Figure 5f. It is to be noted that the wider apart the upper section of the eye, the more the distortion set by the signal to noise ratio and the more the time variation of zero crossing, the smaller the better. This confirms that the signal worsens till its nonexistent as attenuation increase on the fiber cable.
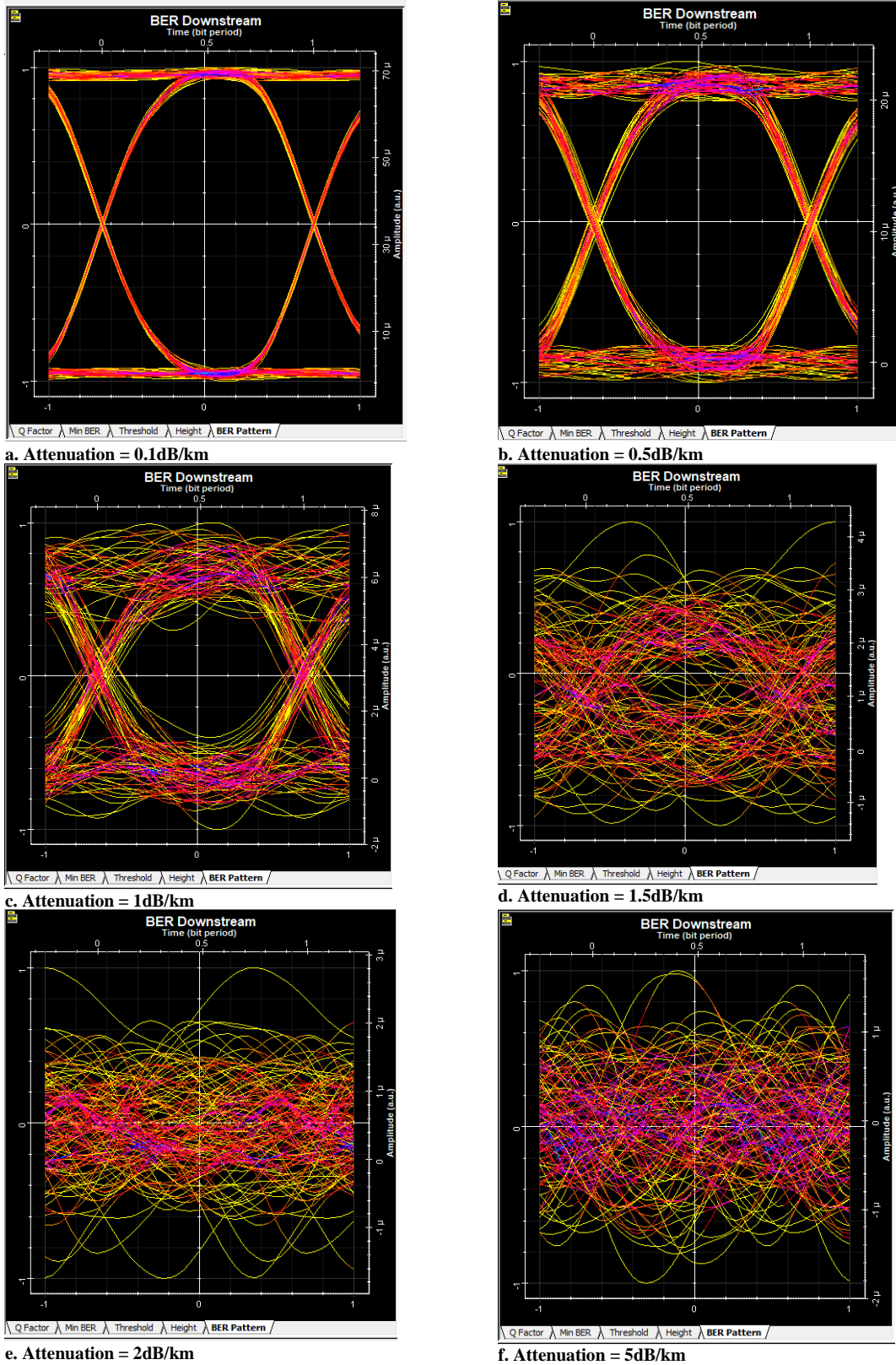
a. Attenuation = 0.1dB/km

b. Attenuation = 0.5dB/km

c. Attenuation = 1dB/km

d. Attenuation = 1.5dB/km

e. Attenuation = 2dB/km

f. Attenuation = 5dB/km

Figure 5. Eye Diagram (GPON OLT - Downstream)

a. Attenuation = 0.1dB/km

b. Attenuation = 0.5dB/km

c. Attenuation = 1dB/km

d. Attenuation = 2dB/km

e. Attenuation = 2dB/km

f. Attenuation = 5dB/km
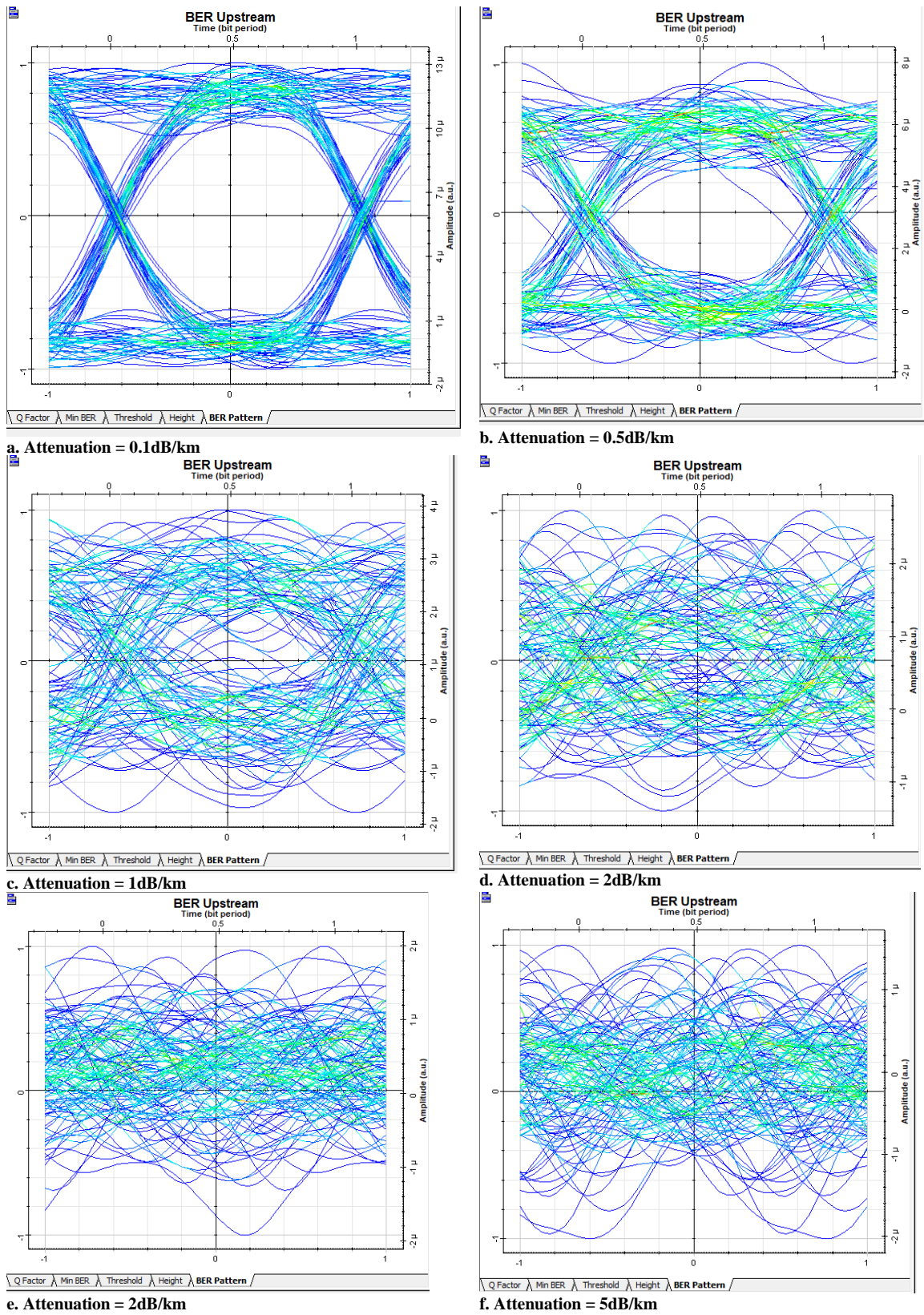
Figure 6. Eye Diagram (GPON ONU - Upstream)
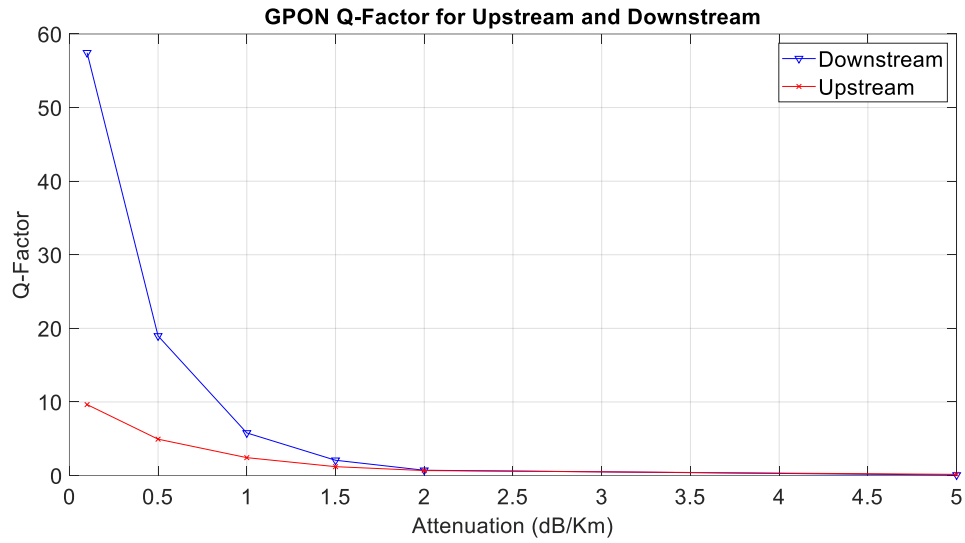
Figure 7. Upstream and Downstream graphs for Q-factor impact vs Attenuation
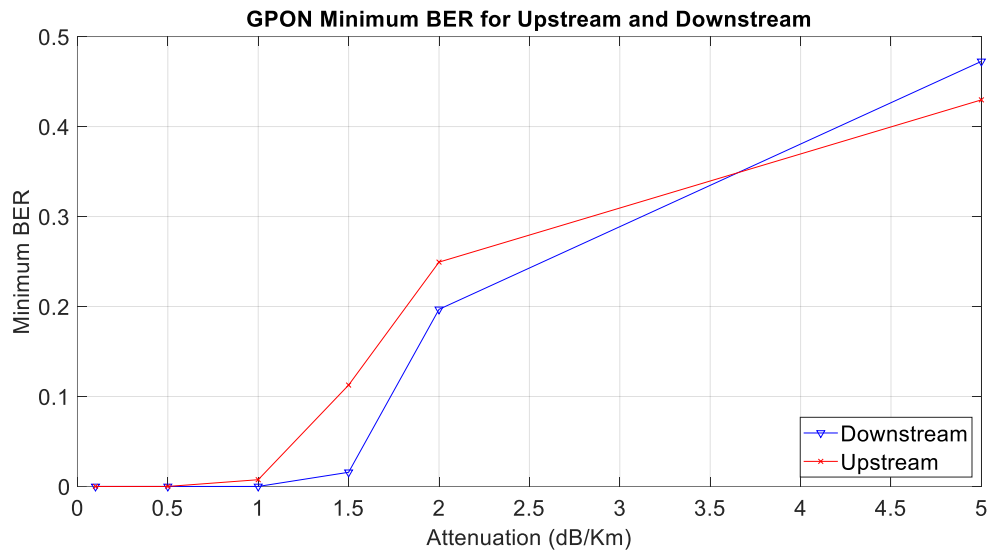
Figure 8. Upstream and Downstream graphs for Minimum BER impact vs Attenuation
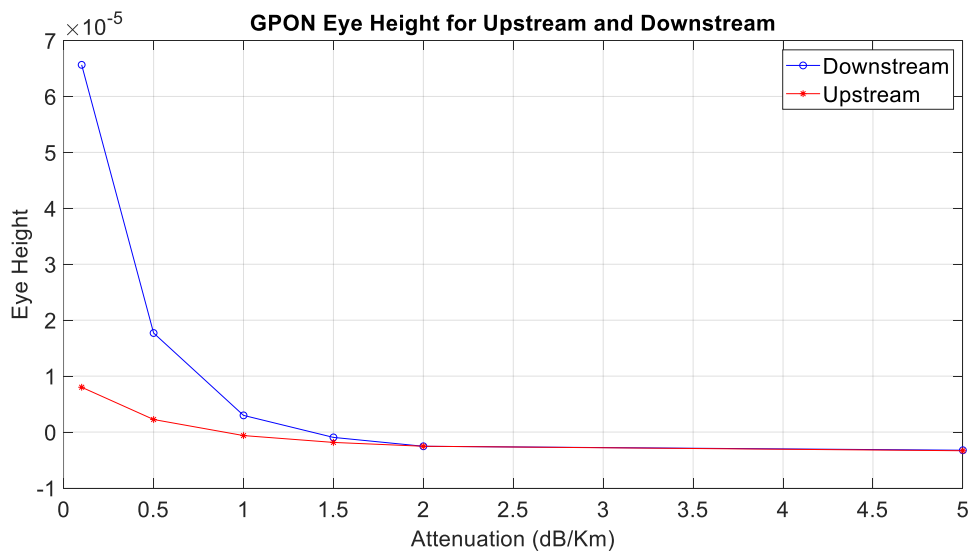
Figure 9. Upstream and Downstream graphs for Eye Height impact vs Attenuation

Figure 10 depicts the Optical power in downstream and upstream data respectively. The optical power is observed to decrease in a similar pattern as the attenuation is increased. This inversely proportional relationship is verified by theory, the higher the attenuation, the lower the optical power at the receiver. The relationship is captured in Figure 10.
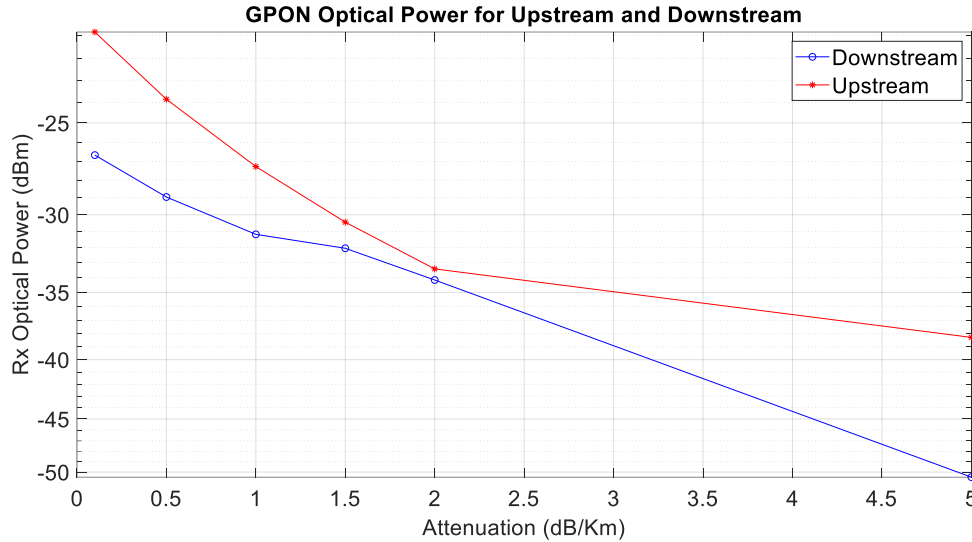

Figure 10. Upstream and Downstream graphs for Rx Optical Power vs Attenuation

Table 3 places side by side the results obtained from the simulated network experiment and that of the live network experiment. It was seen that though cable bending numbered by turns induced the attenuation on the live network, the optical power reduced inversely proportionally to the attenuation coefficient. At two turns of the fiber patch cord, a similar attenuation coefficient was recorded with a similar optical power on both experiments at -26.650 and -26.0 on the simulated and live networks respectively. This pattern continues with very slight variations down the iterations. These variations could be as a result of environmental factors on the live network as no absolute human control could be ascertained over what happens on the outside plant infrastructure during these experiments.

Table 3. Validation of effect of attenuation on optical cable

S/N	No. of Turns	Attenuation Coefficient (dB/km)	Optical Power- Simulated Network (dBm)	Optical Rx Power - Live Network (dBm)
1	2	0.1	-26.650	-26.0
2	3	0.5	-28.963	-27.6
3	4	1.0	-31.190	-31.5
4	5	1.5	-32.065	-32.8
5	6	2.0	-34.150	-34.6

Data from Figure 11, however, shows that the more losses are induced, the more the attenuation coefficient is altered negatively, the less the optical power received at the client's ONU [19] [20]. The less the optical power, the more distorted the quality of signal and the less the performance of the Internet access till a total outage is experienced. This shows the impact of fiber failures on the performance and availability of Internet access over fiber cable. The more fiber cables are protected from bends or attenuation inducing factors such as vibrations, impurities and mechanical stress the better the network performance will be.

The attenuation coefficient of fiber can be 0.36dB/km in wavelength of 1310nm as well as 0.22dB/km in wavelength of 1550nm. This infers that the wavelength of the fiber cable and the distance covered is operationally contributory to the optical power at the client/receiving ONU.
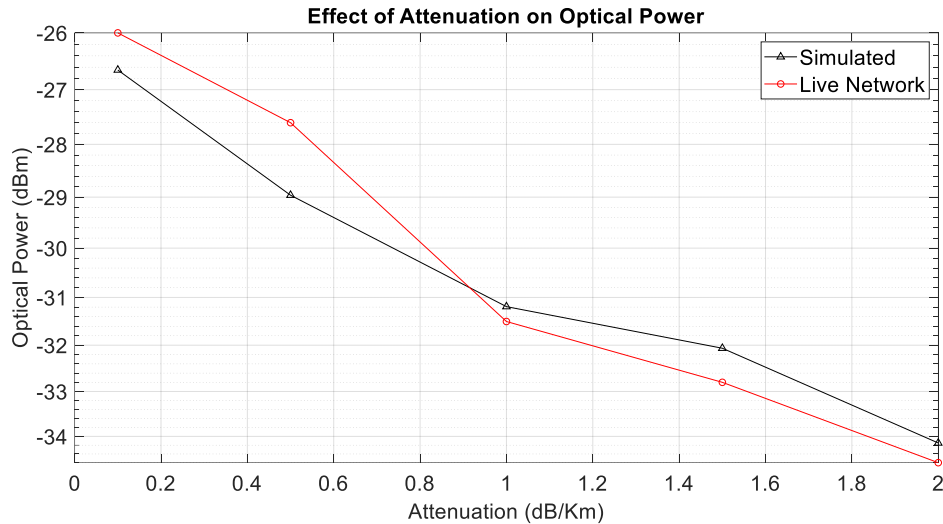
Figure 11. Validation of effect of attenuation on optical cable demonstrated on a simulated GPON FTTH network and live GPON network

In order to curb performance degradation due to fiber cuts, a type-B PON protection with wireless autofailover design has been proposed. This design has full redundancy of the service with the introduction of a point-to-multipoint microwave service with auto failover at the client premise with the platform redundant solution to mitigate total outage on the service is shown in Figure 12. The service works in an active-passive mode, allowing the router to determine the preferred path to the uplink. Its decision making algorithm is strictly based on service availability, however, when both services are up and running, OSPF costing provides preference for the fiber uplink path over the microwave path.

To evaluate the performance of the proposed design in Figure 12, the service protection solution was subjected to induced failures, segment-by-segment of design. The first test was to break the primary backbone fiber cable between the VGC OLT and the first 1:8 splitter, this was achieved by shutting down the PON port serving this cable. A spike in response time of the port-channel serving clients was observed on the real-time monitoring tool to capture the failover from the primary PON port to the secondary PON port. A maximum response time of 4 ms spiked to 80 ms, in 6 seconds. The recovery duration is captured in Figure 13.
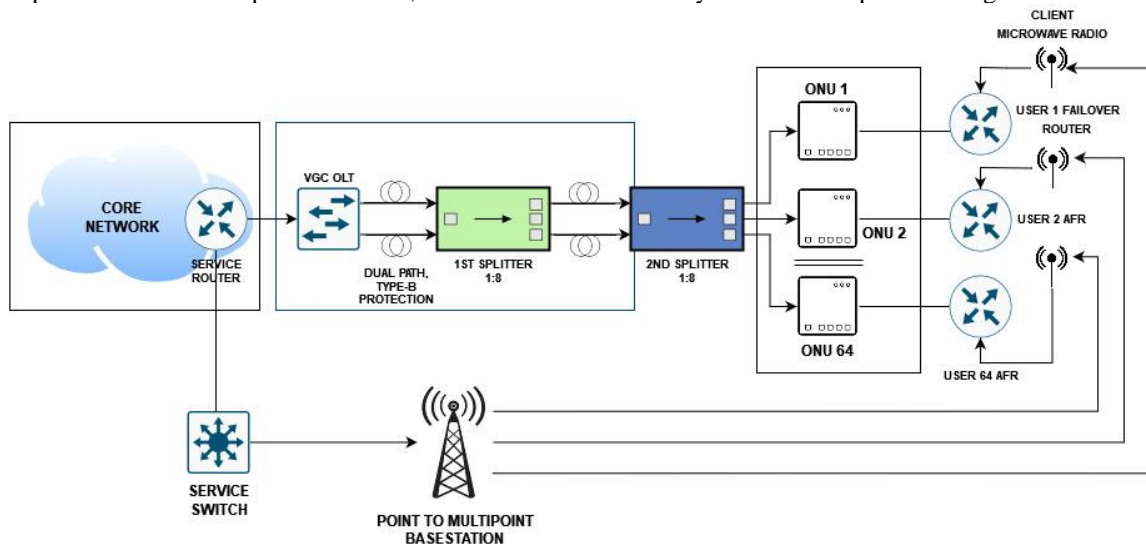

Figure 12. Schematic of proposed design with Type-B PON protection with wireless autofailover option

The second test conducted was a total isolation of the connection between the second 1:8 splitter from the ONU. This was to depict a last mile fiber cut to the ONU. This type of cut eliminates the Type-B PON protection and exposes the client to an imminent outage. This was achieved by shutting down the PON interface of the ONU device.
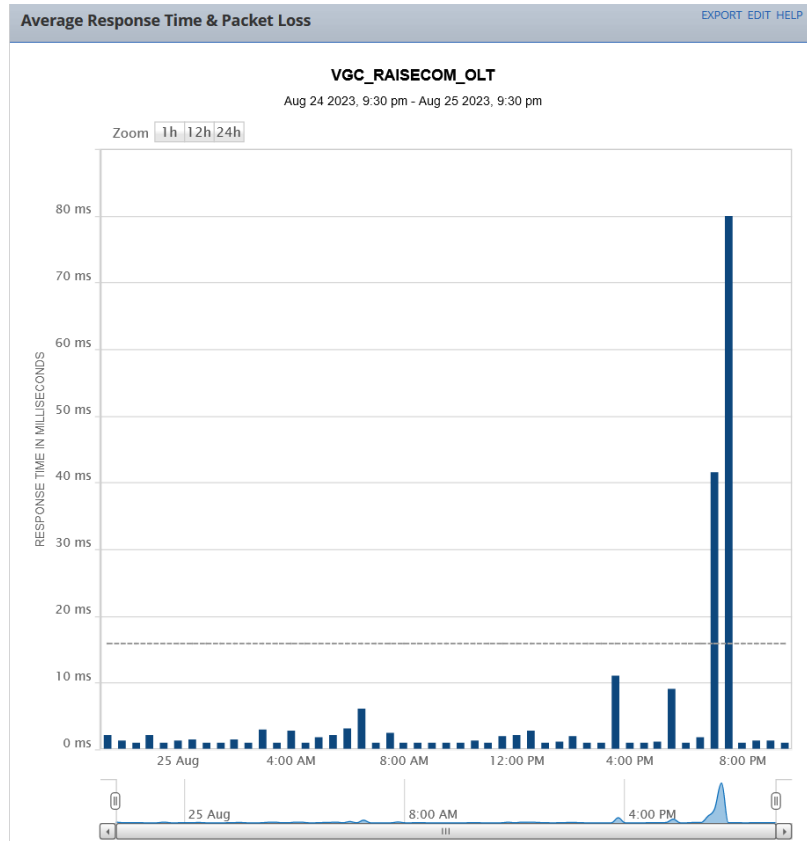
Figure 13. Real-time monitoring of OLT port-channel serving client depicting failover response time spike

Figure 14 shows the aggregate percentage availability during the failover to the alternate platform uplink which is a wireless microwave link. A recovery failover time of 10 secs was observed as shown by a 50% drop on the monitoring tool. The default hello-timer of 10 seconds and dead timer of 40 seconds were adjusted to 5 seconds and 10 seconds respectively to achieve higher availability. According to [21], the results obtained align with previous research conducted. With this, it can be confirmed that an abosultion service protection of cut and service outage can be mitigated.
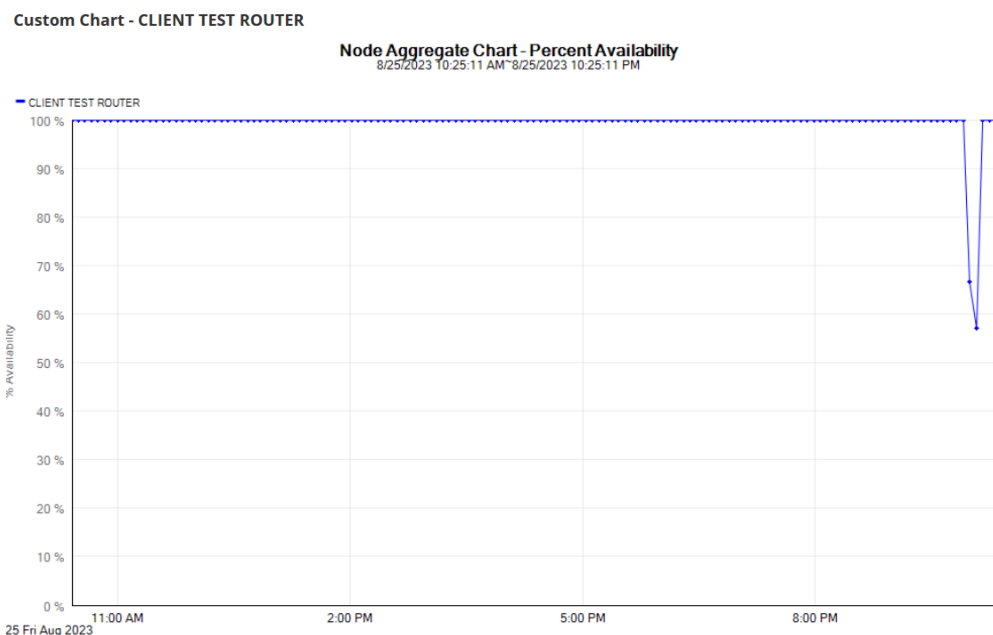

Figure 14. Node aggregate percentage availability chart of live OSPF service recovery during failover

4. CONCLUSION

It is also observed from the experiments conducted on simulated network, validated by the live network experiment that at a similar cable length of 5.4km, the behavior is similar, an increase in attenuation produced decrease in Q-factor, Eye Height, optical power. While an increase in attenuation resulted in an increase in the minimum BER. All results align with theory and corresponds with expectations both on the downstream traffic and upstream traffic. From experiments conducted to observe the technical effects of failures, it was observed that performance generally falls till a total outage is experienced. Q-factor, optical power, minimum BER, and Eye Height all worsens till the service signals are totally gone or unusable at the client premise.

REFERENCES

[1] B. M. Kuboye, "Evaluation of Broadband Network Performance in Nigeria," International Journal of Communications, Network and System Sciences, vol. 10, no. 9, pp. 199–207, 2017.

[2] O. Okoyeigbo, A. E. Ibhaze, A. Olajube, O. Shobayo, T. Somefun, and O. Steve-Essi, "Design and analysis of a broadband microwave amplifier," Indonesian Journal of Electrical Engineering and Informatics, vol. 9, no. 1, pp. 210 – 219, 2021.

[3] O. E. Agboje, S. O. Adedoyin, and C. U. Ndujiuba, "State of Fiber Optic Networks for Internet Broadband Penetration in Nigeria - A Review," International Journal of Optoelectronic Engineering, vol. 7, no. 1, pp. 1–12, 2017.

[4] Nyarko-Boateng, O. et al., "Fiber optic deployment challenges and their management in a developing country: A tutorial and case study in Ghana," Engineering Reports, vol. 2, no. 2, pp. 1–16, 2020.

[5] C. Umezuruike, and A. Oludele, "Broadband Internet Penetration in Nigeria: A Review," International Journal of Research Studies in Computer Science and Engineering, vol. 2, no. 1, pp. 1–7, 2015.

[6] G. N. Ezeh, and O. G. Ibe, "Efficiency of Optical Fiber Communication for Dissemination of Information within the Power System Network," IOSR Journal of Computer Engineering, vol. 12, no. 3, pp. 68–75, 2013.

[7] T. Hayford-Acquah, and B. Asante, "Causes of Fiber Cut and the Recommendation to Solve the Problem," IOSR Journal of Electronics and Communication Engineering, vol. 12, no. 01, pp. 46–6, 2017.

[8] NCC, Subscriber/Network Data Report. Nigerian Communication Commission, 2020.

[9] A. E. Ibhaze, F. O. Edeko, and P. E. Orukpe, "A signal amplification-based transceiver for visible light communication," Journal of Engineering, vol. 11, no. 26, pp. 123 – 132, 2020.

[10] A. E. Ibhaze, P. E. Orukpe, and F. O. Edeko, "High Capacity Data Rate System: Review of Visible Light Communications Technology," Journal of Electronic Science and Technology, vol. 18, no. 3, 100055, 2020.

[11] W. D. Grover, "Mesh-Based Survivable Networks: Options and Strategies for Optical, MPLS, SONET, and ATM Networking," Upper Saddle River, NJ, Prentice Hall PTR, 2003.

[12] D. Crawford, "Fiber Optics Cables Dig-Ups - Causes and Cures," MCI Telecommunication Corporation, pp. 1–32, 1993.

[13] Agrawal, G. P, "Fiber-optic Communication Systems," John Wiley & Sons, New York, 2nd edition, pp. 490-495, 1997.

[14] J. C. Cartledge, G .S. Burley, "The Effect of Laser Chirping on Lightwave System Performance," Journal of Lightwave Technology, vol. 7, no. 3, S. 568-573, 1989.

[15] C. J. Anderson, J. A. Lyle, "Technique for evaluation of systems performance using Q in numerical simulation exhibiting intersymbol interference," Electronic Letters, vol. 30, no. 1, S. 71-72, 1994.

[16] P. A. Humblet, "On the Bit Error Rate of Lightwave Systems with Optical Amplifiers," Journal of Lightwave Technology, vol. 9, no. 11, pp. 1576–1582, 1991.

[17] D. Marcuse, "Calculation of Bit-Error Probability for a Lightwave System with Optical Amplifiers and Post-Detection Gaussian Noise," Journal of Lightwave Technology, vol. 9, no. 4, pp. 505–513, 1991.

[18] D. Marcuse, "Derivation of Analytical Expressions for the Bit-Error Probability in Lightwave Systems with Optical Amplifiers," Journal of Lightwave Technology, vol. 8, no. 12, pp. 1816–1823, 1990.

[19] M. S. Ab-Rahman, L. Al-Hakim Azizan, S. A. C. Aziz, K. Jumari. "The Eye Diagram Analysis of Restoration Scheme in FTTH-PON," Journal of Applied Sciences, vol 11, no. 5, pp: 840-847, 2011.

[20] W. M. Osman, K. H. Billal, and A. B. Al-Nabi, "Bit Error Rate Performance for Optical Fiber System," Journal of Electrical & Electronic Systems, vol. 7, no. 1, 1000250, 2018.

[21] J Panford, E. Asabere, J. Hayfron-Acquah, "Comparative Analysis Of Convergence Times Between OSPF, EIGRP, IS-IS and BGP Routing Protocols in a Network," International Journal of Computer Science and Information Security (IJCSIS), vol. 15, no. 12, 2017.